



Maximum Channel Access Probability Based on Post-Disaster Ground Terminal Distribution Density

Xingxing Hu^{1,2(✉)}, Demin Li^{1,2(✉)}, Chang Guo^{1,2}, Wei Hu^{1,2}, Lei Zhang^{1,2},
and Menglin Zhai^{1,2}

¹ College of Information Science and Technology, Donghua University,
Shanghai 201620, China

2181295@mail.dhu.edu.cn, deminli@dhu.edu.cn

² Engineering Research Center of Digitized Textile and Apparel Technology,
Ministry of Education, Shanghai 201620, China

Abstract. In post-disaster relief, how to design an efficient emergency communication system (ECS) to provide emergency communication service and improve channel access probability still remains a challenge. In this paper, we use Thomas cluster process (TCP) to model the locations of ground terminals (GT) and propose a new scheme to maximize channel access probability. The proposed emergency communication infrastructure includes a hovering helicopter and a Unmanned Aerial Vehicle (UAV) to provide communication service for GTs. Different from the existed work, an adaptive speed cruise model is proposed for the UAV depending on distribution density of GTs. Then, an efficient dynamic channel resource schedule method is proposed for system with limited channel resource. The channel access probability is formed as non convex optimization problem. The original non-convex optimization problem is transferred into a convex problem by analyzing objective function. An interior-point method is adopted to solve this problem. Extensive simulations are performed to evaluate the model by optimizing the UAV speed in different regions. The results show that the proposed new scheme outperforms the one with constant cruise speed for UAV and static scheduling for channel resource allocation.

Keywords: Channel access probability · UAV · Ground terminal distribution density · TCP · Adaptive speed cruise · Resource schedule

1 Introduction

In order to quickly establish an efficient and reliable ECS, UAV has been used to assist emergency communication in [1]. The three typical cases of UAV-assisted wireless communication, including aerial base station (BS), relay [2] and information dissemination and data collection [3], are discussed in [4]. Researchers have done a lot of works based on these three application scenarios.

In [5], authors are the first to propose a novel 3-D UAV-BS placement to maximize the number of covered users with different quality-of-service (QoS) requirements. They modeled the placement problem as a multiple circles placement problem and a low-complexity maximal weighted area algorithm was also proposed. In [6], authors adopted an air-to-ground (A2G) channel model that incorporated line-of-sight (LoS) and non-line-of-sight (NLoS) propagation. Channels experienced Rayleigh and Nakagami-m fading in the UAV-BSs network, respectively. The variation trend of average achievable rate with UAV distribution density was also analyzed and the results revealed that the coverage probability and average achievable rate decreased as the height of the UAV-BSs increased. In [7], an aerial network formed by multiple UAVs for assisting data relaying in disaster recovery was studied. The coverage probability of down-link user was analyzed and the optimal altitude of UAVs was achieved to maximize the capacity of ground network. However, the recent researches focus on the single factors. The model that considers both channel state and assignment is seldom studied.

In [8], an UAV was deployed to provide the fly wireless communication in a given geographical area. The system average coverage probability and sum-rate were analyzed when UAV was static and mobile, respectively. By using the disk covering problem and minimizing the number of stop points that the UAV needed to visit in order to completely cover the area, the minimum outage probability was obtained. In addition, in order to provide full coverage for the area of interest, the tradeoff between coverage and delay was discussed. In [9], Zhang *et al.* proposed a novel scenario that the service area was divided into two parts and covered by two UAVs, respectively. The difference from previous research is that authors took the channel access delay for establishing a full transmission between the vehicle and UAV into account. The coverage probability and achievable rate of a random vehicle located in the served area were derived by geometric analysis. Through changing related parameters, the optimal setting for the maximum coverage probability and achievable rate was obtained.

There are some problems need to be further optimized. First, the impact levels in the whole post-disaster area maybe different. More severely affected areas could become hotspots and a TCP is more suitable to model the locations of GTs rather than a Poisson point process (PPP). Second, UAV speed should be adjusted when it cruises the served area. According to the GT distribution densities of different regions, UAV should dynamic adjust its speed to increase the successfully access probability of each GT. Finally, a dynamic channel resource schedule should be made to further improve channel access. Different GT distribution densities require a flexible channel schedule constantly between aerial base stations. Above all, the contributions of this paper are listed as follows.

- First, in post-disaster area, a more suitable TCP rather than PPP is used to model the locations of GTs and each cluster has different GT distribution density. We propose an UAV adaptive speed cruise model based on GT distribution density.

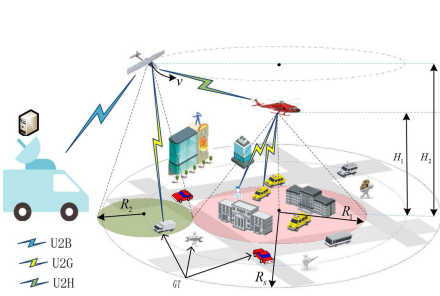


Fig. 1. Illustration of system model.

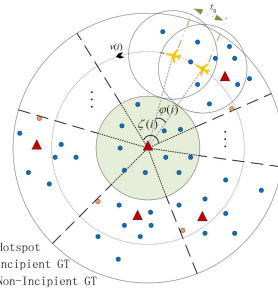


Fig. 2. Illustration of cruise model.

- Second, combining with channel state, we discuss the system channel access probability based on the channel resource availability. An efficient channel schedule method is proposed to alleviate resource competition.
- Finally, through transferring objective function and making mathematical approximations, the original non-convex problem is transformed into convex problem. The simulation results show the proposed new scheme achieves maximum channel access probability compared with the constant UAV cruise speed and static channel resource schedule.

2 System Model

2.1 Network Structure and GT Distribution

In order to quickly establish a local ECS, a hover flying helicopter (HFH) and an UAV are deployed to cover the worst heavily hit area and others, respectively. As shown in Fig. 1, according to the affected area and coverage of HFH and UAV, a local ECS is established to serve a circular post-disaster area with radius R_s . HFH's coverage is a circular area with radius R_1 . The cruise flying UAV circles around HFH and its coverage is also a circle with radius R_2 . By adjusting aircrafts' transmission powers or flight altitudes, the coverage of HFH and UAV is neither overlap nor gap. In order to ensure that GTs located on the edge of served area can be also covered, $R_s - (R_1 + 2R_2) \geq o$, where $0 \leq o \ll R_2$. Compared with center area, the other regions are less heavily hit. An UAV can be deployed quickly and efficiently scan those area to provide communication service for GTs. HFH and UAV can also communicate by H2U(U2H) link to exchange messages, such as adjusting both sides' coverage, and connect to the outside world through themselves or another one.

There would be many GTs in the ground of disaster area and all GTs are equipped with battery powered transceivers. These GTs mainly include emergency rescue vehicles, communication equipments of search and rescue personnel, phones of trapped person, sensors for environmental monitoring and so on. In general, densely populated areas, such as schools, hospitals, dwelling districts and so on, are more likely to be hotspots and need more emergency service after the

impact of disaster. Thus, Poisson cluster process (PCP) [10] is more suitable to describe the location distribution of those hotspots and GTs. Based on the above analysis, the locations of hotspots are modeled by an independent PPP of density $\lambda^{hs} > 0$. And the locations of all GTs who are scattered around hotspots are modeled by a TCP. Unlike cellular network whose service areas are overlapping and complex, we assume these clusters are scattered and do not overlap. Thus, the probability density function (PDF) of TCP based scattered UEs around hotspot l with random distance vector Z , $f_Z(z) = \frac{1}{2\pi\sigma_{t,l}^2} \exp(-\frac{z^2}{2\sigma_{t,l}^2})$, $z \in \mathbb{R}^2$,

where $\sigma_{t,l}$ is the variance of cluster l formed by TCP. The distance from a GT to the center of cluster l is denoted as D . Then the distribution of D can be expressed as $\bar{F}_D(x) = \exp(-\frac{x^2}{2\sigma_{t,l}^2})$, $x \geq 0$.

In our model, the impact level is different among the whole post-disaster area and the area covered by HFH is the worst heavily hit one. Therefore, the GTs densities among disaster area are also different. In Fig. 2, the disaster area covered by UAV is divided into I sector rings according to the clusters' locations. The beginning and ending bounds of sector ring are defined as the locations when UAV covers a cluster for the first time until it covers another. Incipient GT is the first one to be served in the cluster that UAV is going to serve. The average number of GTs in cluster i is \mathcal{N}_i , where $i = 1, \dots, I$ and \mathcal{N}_0 for the HFH served cluster. We denote ζ_i (radian) as the central angle of sector ring i . In addition, considering the geometry, ζ_i satisfies $\sum_{i=1}^I \zeta_i = 2\pi$.

2.2 Channel Model

In this paper, we consider the Air-to-Ground channel which is dominated by Light-of-Sight (LoS) [11] links and the random access mechanism in MAC layer is adopted, such as IEEE 802.11 distributed coordination function protocol. When the HFH and UAV implement communication coverage, the SNR of ground terminal (GT) receiver must be greater than a threshold. Therefore, We use $g_j(r, \beta)$ [12] to represent the channel power gain of the communication link between the GT and HFH or UAV, $g_j(r, \beta) = \frac{\beta \cdot \beta_0}{H_j^2 + r^2}$, where β is the small scale fading in a certain distribution which subjects to Gamma distribution, β_0 denotes the channel power at the reference distance 1 m, H_j is the flying height of HFH or UAV ($j = 1, 2$, for the HFH and UAV, respectively). And r is the distance from GT to the horizontal projection point of the HFH or UAV. The channels in our model used are orthogonal. By this way, interference between channels is not considered. Thus, when implementing communication coverage, the SNR of the GT receiver must be greater than a threshold

$$SNR_j(\beta, r) = \frac{W_j \cdot g_j(r, \beta)}{\sigma^2} \geq \gamma_0, \quad (1)$$

where W_j is transmission power of aircraft j , σ^2 is the noise power of receiver, γ_0 is the SNR threshold.

2.3 Cruise Model

In our cruise model, the HFH hovers at a height H_1 above the central axis of the circular disaster zone. When UAV serves cluster i , it will adjust its speed to improve its quality of service. When UAV finishes its service for current cluster, it will maintain this speed $v(i)$ until it serves another cluster. With reference to the literature [13], we introduce the channel access delay t_0 (*seconds*) which indicates the minimum time for establishing a complete communication link with the UAV is t_0 . Based on this assumption, within the time t_0 , an overlapping area will appear as shown in Fig. 2. Only GTs in this overlapping area can establish complete communication links with the UAV. Since the UAV is fixed-wing, according to aerodynamics, it needs a certain speed to maintain it aloft, we denote by V_{min} and V_{max} the minimum and maximum speed of it, respectively. $\varphi(i)$ denotes the central angle of sector formed when UAV flies along the trajectory within time t_0 . According to stochastic geometry analysis, the relation between $\varphi(i)$ and $v(i)$ is $\varphi(i) = \frac{v(i) \cdot t_0}{R_{12}}$, and $v(i) \leq V_{max}^a$, where $R_{12} = R_1 + R_2$. When the coverage area of UAV in time t is tangent to that in time $t + t_0$, V_{max}^a can be expressed as $V_{max}^a = \min(V_{max}, \frac{2R_{12}}{t_0} \sin^{-1}(\frac{R_2}{R_{12}}))$.

3 Problem Formulation and Analysis

3.1 Channel SNR Threshold Probability

Considering the channel state information (CSI), we introduce a SNR threshold probability $P_{T,j}$ which is defined as the probability that a random GT satisfies the SNR condition when it picks up the detection signal sent by its corresponding aircraft j . The detail expression is

$$P_{T,j} = \mathbb{E}_r \left[\mathbb{P} \left(\frac{W_j \cdot g_j(r, \beta)}{\sigma^2} \geq \gamma_0 \mid r \right) \right]. \quad (2)$$

In order to obtain the specific expression of $P_{T,j}$, we need to figure out the probability density function (PDF) of r .

First, it is necessary to calculate the area $S(i)$ of overlapping region when UAV flies over the sector ring i . As mentioned above, we assume $o \ll R_2$ to ensure GTs located on the edge of disaster area can be also covered. For simplicity of calculation, we assume $R_s \approx R_1 + 2R_2$ when o is very small. Thus, according to geometry, $S(i)$ can be approximated by

$$S(i) \approx 2R_2^2 \cos^{-1} \left(\frac{R_{12} \cdot \sin \frac{\varphi(i)}{2}}{R_2} \right) - 2R_{12} \sin \frac{\varphi(i)}{2} \sqrt{R_2^2 - R_{12}^2 \sin^2 \frac{\varphi(i)}{2}}. \quad (3)$$

Based on reference [9], under the coverage of HFH, $f_{d_1}(r)$ denotes the PDF of r . It can be easily derived as $f_{d_1}(r) = 2r/R_1^2$ and the upper bound of r is R_1 . Under

the coverage of UAV, there are two geometric cases. By drawing the circle with radius r whose center is midpoint of the UAV trajectory during t_0 , we denote by $f_{d_2}^i(r)$ the PDF of r , $f_{d_2}^i(r) = 2\pi r/S(i)$ and $0 \leq r \leq R_2 - R_{12} \sin \frac{\varphi(i)}{2}$.

In our proposed channel model, the total bandwidth B is divided into M orthogonal channels. By this way, interference between channels is not considered. In the case of small-scale fading, we choose Nakagami- m distribution. And its shape parameter s determines what distribution the channel obeys. According to the literature [13], the channel fading power gain β is subject to Gamma distribution and its PDF can be expressed as $f_g(\beta) = \frac{s^s \beta^{s-1}}{\Gamma(s)} e^{-s\beta}$,

where $\Gamma(s) = \int_0^\infty x^{s-1} e^{-x} dx$. $s = \frac{N^2 + 2N + 1}{2N + 1}$ and N is a constant.

3.2 Channel Schedule and Cruise Efficiency

In terms of channel schedule, we assume there are M orthogonal channels that do not interfere with each other. η_i denotes the percentage of channels obtained by HFH when the UAV flies over the sector ring i . So, it is $1 - \eta_i$ for the UAV and the total channel number obtained by HFH and UAV are $\eta_i \cdot M$ and $(1 - \eta_i) \cdot M$, respectively. η_i is changeable when UAV flies over different areas because of the different GT distribution density.

We denote λ_i as the GT density of cluster i covered by UAV and λ_0 for center cluster covered by HFH, respectively. Considering the communication access threshold t_0 , only GTs in the overlapping area covered by UAV and the area covered by HFH can communicate with the corresponding aircraft.

Lemma 1. *When $\overline{F}_D(x^*) \leq \rho$, we assume all GTs clustered around its corresponding hotspot are located in the circle of radius x^* .*

Proof. In theory, GTs located in the cluster formed by TCP could appear anywhere away from center hotspot. And the only matter is the smaller and smaller probability when GT is gradually far away from hotspots. And this probability would approach to 0 when the distance is far enough. In practice, this limiting case is not going to happen. For example, in order to guarantee his normal work, a rescuer with communication equipment will not be too far from the hotspot. Then, emergency communication services is a kind of opportunistic access and we can not guarantee 100% completely coverage for all GTs. When $\overline{F}_D(x^*) \leq \rho$, this error is within our acceptable range and x^* is the farthest distance from GT to its cluster center.

According to the average number of GTs of each cluster, the GT density of cluster i covered by UAV can be given by $\lambda_i = \frac{\mathcal{N}_i}{\pi \cdot x_i^2}$, $i = 1, \dots, I$. Considering GTs covered by HFH can establish uninterrupted communication links with HFH, there is not necessary to analysis the GT density in this cluster. Thus,

when UAV serves cluster i , the detailed expression of η_i is presented as following formula $\eta_i = \frac{\mathcal{N}_0}{S(i) \cdot \lambda_i + \mathcal{N}_0}$. By dynamically adjusting η_i , it can effectively alleviate the channel resource competition between HFH and UAV when UAV serves different clusters.

As mentioned in the above section, it is necessary to consider the cruise efficiency of UAV. We denote by T_i the time that the UAV flies past the sector ring i at the speed $v(i)$ and the time constraint for the whole system is given as $\sum_{i=1}^J T_i \leq T_c$, where $T_i = \frac{\zeta(i) \cdot R_{12}}{v(i)}$ and T_c is a constant that denotes the duration of cruise cycle.

3.3 Maximum Channel Access Probability

When UAV serves cluster i , we denote by $P^U(i)$ the probability that a typical GT located in the cluster i can successfully connect to the UAV, and by $P^H(i)$ the probability that to the HFH. Thus, when UAV serves cluster i , the channel access probability is

$$P(i) = \sum_{\kappa=1}^I [P_{T,1} \cdot P^H(i) + P_{T,2}(i) \cdot P^U(i)] \cdot \delta(\kappa - i). \quad (4)$$

$\tau^H(i)$ and $\tau^U(i)$ are used to represent the probability that a GT covered by HFH or UAV when UAV flies over the sector ring i , respectively. And they can be expressed as following formulas

$$\tau^H(i) = \frac{2\pi R_1^2}{2\pi R_1^2 + \zeta(i)(R_s^2 - R_1^2)}, \quad \tau^U(i) = \frac{2S(i)}{2\pi R_1^2 + \zeta(i)(R_s^2 - R_1^2)}. \quad (5)$$

In practice, because of limited channel resource, there will be competition for it. Assuming the number of channels is less than or equal to the number of GTs. And GTs in different cluster, even in the same one, will also fiercely compete for limited channel resource. Based on the above analysis, therefore, we define two variables denoted by $C^H(i)$ and $C^U(i)$ whose meanings are the number of channel per GT located in the clusters covered by the HFH and UAV, respectively. And the detailed expressions are presented as

$$C^H(i) = \frac{\eta_i M}{\mathcal{N}_0}, \quad C^U(i) = \frac{(1 - \eta_i) M}{\lambda_i \cdot S(i)}. \quad (6)$$

When UAV flies past sector ring i and then serves cluster i , the channel access probability $P(i)$ can be rewritten as

$$\begin{aligned}
 P(i) &= \sum_{\kappa=1}^I [P_{T,1} \cdot P^H(i) + P_{T,2}(i) \cdot P^U(i)] \cdot \delta(\kappa - i) \\
 &= \sum_{\kappa=1}^I \left[P_{T,1} \cdot \tau^H(i) \cdot C^H(i) \right. \\
 &\quad \left. + P_{T,2}(i) \cdot \tau^U(i) \cdot C^U(i) \right] \cdot \delta(\kappa - i).
 \end{aligned} \tag{7}$$

Thus, when the UAV completes a cruise cycle, the system average channel access probability P is given as $P = \frac{1}{I} \sum_{i=1}^I P(i)$.

Now, our objective function can be expressed as

$$\begin{aligned}
 P1 : \max_{v(i)} \quad & P \\
 \text{s.t.} \quad & (18), \\
 & V_{min} \leq v(i) \leq V_{max}^a.
 \end{aligned} \tag{8a}$$

$$\tag{8b}$$

3.4 Problem Analysis

It is obvious that the first and second term of $P(i)$ are both related to $v(i)$. First, we consider the first term of $P(i)$. Because the numerator of the first term is a constant which is not related with $v(i)$, therefore, the first term can be simplified

$$\text{as } \Upsilon_1(i) = \frac{1}{S(i) \cdot \lambda_i + \mathcal{N}_0}$$

Lemma 2. *There exists a unique $v^*(i)$ to make $\Upsilon_1(i)$ convex when $v(i) \leq v^*(i)$.*

Proof. First, taking $\varphi(i)$ as our variable to obtain the first-order and second-order derivatives of $\Upsilon_1(i)$ which are expressed in following formulas

$$\Upsilon_1'(i) = \frac{-\lambda_i S'(i)}{(\lambda_i S(i) + \mathcal{N}_0)^2}, \quad \Upsilon_1''(i) = \frac{\lambda_i [\lambda_i S(i) + \mathcal{N}_0] \cdot L_1(\varphi(i))}{(\lambda_i S(i) + \mathcal{N}_0)^4} \tag{9a}$$

where $L_1(\varphi(i)) = 2\lambda_i [S'(i)]^2 - S''(i) [\lambda_i S(i) + \mathcal{N}_0]$. It's easy to prove that $L_1(\varphi(i))$ is a monotonous non-increasing function and $L_1(0) > 0$, $L_1(\pi) < 0$. In fact, $\varphi(i)$ is much less than π . According to the monotony of the function, we can conclude that there is bound to be a speed $v^*(i)$ to make $L_1 = 0$. And $v^*(i)$ can be found by binary search algorithm. When $v(i) \leq v^*(i)$, the $L_1 \geq 0$, so as $\Upsilon_1''(i)$. Therefore, $\Upsilon_1(i)$ is convex.

Now, we consider the second term of $P(i)$ and rewrite the variables related with $v(i)$ as $\Upsilon_2(i) = \frac{Q(\varphi(i))}{S(i) \cdot \lambda_i + \mathcal{N}_0}$, where the details of $Q(\varphi(i))$ can be seen from following proof.

Algorithm 1. Interior point method solution for $P1$

Input: $\zeta(i)$: The central Angle of sector i ; t : step length; μ : scale factor; ϵ_1, ϵ_2 : error thresholds; β_1 :backtracking line search parameter

Output: optimal \mathbf{V}

- 1: initial $r^{(0)} = 1, m = 0, V^{(0)}$
- 2: **repeat**
- 3: **repeat**
- 4: calculate Newton step_path ΔV_{nt} and decrement ℓ^2
 $\Delta V_{nt} = -\nabla^2 \chi_2(V^{(m)}, r^{(m)})^{-1} \nabla \chi_2(V^{(m)}, r^{(m)})$;
- 5: $\ell^2 = \nabla \chi_2(V^{(m)}, r^{(m)})^T \nabla^2 \chi_2(V^{(m)}, r^{(m)})^{-1} \cdot \nabla \chi_2(V^{(m)}, r^{(m)})$;
- 6: update step length: $t = t \cdot \beta_1$
- 7: update $V^{(m+1)} = V^{(m)} + t \cdot \Delta V_{nt}$
- 8: update $\mathbf{V} = V^{(m+1)}$
- 9: **until** $\ell^2 \leq \epsilon_2$
- 10: $r^{(m+1)} = \mu \cdot r^{(m)}$
- 11: **until** $\|V^{(m+1)} - V^{(m)}\| < \epsilon_1$
- 12: **return** \mathbf{V}

Lemma 3. Combining lemma 1, the $\mathcal{Y}_2(i)$ is also convex when $\frac{\beta_0 W_2}{\sigma^2} \geq 2R_2^2 \cdot \gamma_0$.

Proof. Taking $\varphi(i)$ as our variable to obtain the second-order derivative of $\mathcal{Y}_2(i)$ and we can get $\mathcal{Y}_2''(i) = \frac{L_2(\varphi(i))}{[\lambda_i S(i) + \mathcal{N}_0]^3}$, where

$$\begin{aligned} L_2(\varphi(i)) &= \left[Q''(\varphi(i))(\lambda_i S(i) + \mathcal{N}_0) - \lambda_i Q(\varphi(i))S'(i) \right] \\ &\quad \times (\lambda_i S(i) + \mathcal{N}_0) - 2\lambda_i(\lambda_i S(i) + \mathcal{N}_0) \cdot S(i) \\ &\quad \times \left[Q'(\varphi(i))(\lambda_i S(i) + \mathcal{N}_0) - \lambda_i Q(\varphi(i))S'(i) \right], \end{aligned} \quad (10)$$

and $Q(\varphi(i)) = 1 - e^{-\frac{\gamma_0 \cdot \sigma^2}{\beta_0 W_2} (R_2 - R_{12} \sin \frac{\varphi(i)}{2})^2}$. When $\frac{\beta_0 W_2}{\sigma^2} \geq 2R_2^2 \cdot \gamma_0$, $Q(\varphi(i)) \leq 0$.

Now, we define two auxiliary functions to make further analysis of the two terms of $L_2(\varphi(i))$

$$\begin{aligned} h_2 &= -\lambda_i Q(\varphi(i))S'(i) \cdot [\lambda_i S(i) + \mathcal{N}_0], \\ h_3 &= 2\lambda_i S'(i)Q'(\varphi(i)) \cdot [\lambda_i S(i) + \mathcal{N}_0]. \end{aligned} \quad (11a)$$

It is obviously that h_2 and h_3 are both greater than 0. By scaling, $Q'(\varphi(i)) < \frac{\gamma_0 \cdot \sigma^2}{W_2} \cdot (R_2 - R_{12} \sin \frac{\varphi(i)}{2})$. In addition, combining the physical significance of $\frac{\gamma_0 \cdot \sigma^2}{\beta_0 W_2}$ that it is a very small number. So, $Q(\varphi(i))$ can be approximated to $\frac{\gamma_0 \cdot \sigma^2}{\beta_0 W_2} \cdot (R_2 - R_{12} \sin \frac{\varphi(i)}{2})^2$ by Taylor formula. Then, $h_2 > h_3$ is easy to conclude. Therefore, $L_2(\varphi(i)) > 0$ and $\mathcal{Y}_2(i)$ is convex.

Based on the above analysis, the first and second term of $P(i)$ are both convex. According to convex optimization theory, it is easy to confirm that $P(i)$ is also convex. Next, the interior point method and Newton method are used to solve the problem and obtain the optimal solution. $\chi_2(\mathbf{V}, r^{(m)})$ denotes the penalty function of problem $P1$ and the details are presented in Algorithm 1.

4 Simulation

4.1 Parameters Settings

Setting the flight height of HFH and UAV as 100 m and 200 m. The covering radius R_1 and R_2 are set as 450 m, 350 m, respectively. The whole disaster area is divided into 5 subregions which means $I = 5$. And the corresponding central angles are $[\pi/2, \pi/3, \pi/3, \pi/3, \pi/2]$ (radian). The variances $\sigma_{t,1} \sim \sigma_{t,5}$ are set as 65, and 85 for the center cluster covered by HFH, respectively. The average numbers of GTs for cluster 1–5 are set as 11, 13, 11, 15, 13, and 44 for center one, respectively. t_0 is set as 1 s and V_{max} and V_{min} are 80 m/s, 3 m/s. $b = 5$ Hz and other constants, such as $\mu, \varrho, \beta_1, \sigma_{t,0}, \sigma_{t,I}, \epsilon_1, \epsilon_2$ are set as 0.1, 10^{-6} , 0.8, 85, 65, 10^{-6} , 10^{-6} , respectively.

4.2 Results Analysis

It can be seen from Fig. 3 that i): the maximum of $v(i)$ is more than 40 m/s and this increase of speed will be cut in other subregions. ii): the speeds of subregions whose center angles are identical are also tend to be different. In general, the UAV speed will increase with the increase of λ_i . For the first problem, we notice that UAV need to slow down in several subregions to improve channel access probability and speed up in other areas to satisfy the limitation of cruise cycle. Because of the larger center angles of subregion 1 and 5, speeding up in these two subregions will generate more benefit. Aimed to illustrate the second problem, we should review our objective function from global perspective to realize the fact that channel access probability will increase with the decrease of $v(i)$. First, greater λ_i means more GTs, which will lead to fiercer channel competition. Acceleration will reduce the amount of GTs served in each t_0 . Thus, channel competition will be alleviated and the QoS is improved, so as channel access probability. Second, system will adjust the UAV speed of each subregion to achieve maximum channel access probability.

In Fig. 4, there are four maximum channel access probabilities under different conditions: constant speed and η which are adopted in [9], optimized η , optimized UAV speeds, optimized UAV speeds and η . First, when only the UAV speeds are optimized, the increment of channel access probability is 3.4% compared with [9]. Second, optimizing UAV speeds achieves 0.2% improvement when η is already optimized. The reason for this problem is that the UAV speed we used for non-optimized case is close to the optimal speed. Then, these two cases all achieve suitable channel schedule. Thus, the difference between these two increments is not vary distinct. Third, compared with constant channel schedule, the channel

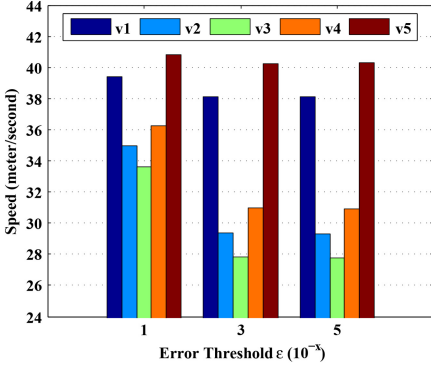


Fig. 3. The speeds of subregions under different error thresholds ϵ

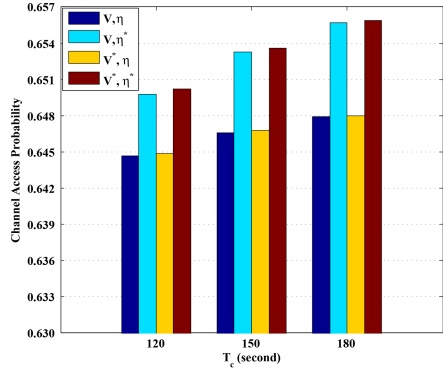


Fig. 4. The channel access probability under different optimization conditions.

access probability is distinctly improved by optimizing η . Fourth, when cruise cycle T_c increases, the channel access probability will increase correspondingly. It's easy to illustrate that UAV will have more time to establish more full communication links when T_c increases. Overall, all those channel access probabilities are less than the probability we can get at the V^* and η^* .

5 Conclusion

In this paper, we propose an adaptive UAV speed cruise model to provide communication service in post-disaster relief. TCP is introduced to model the location distribution of GTs, which is more suitable than PPP. By taking the channel state into account, we discussed the maximum channel access probability of the system under the condition of limited channel resources. And a flexible channel schedule was proposed to improve channel access probability. Simulation results show that channel access probability can be improved by adopting a dynamic channel schedule and optimizing the UAV speed of each subregion. Moreover, compared with constant UAV speed or channel schedule, the simulation results reveal that the proposed method performs well in coverage probability and achievable rate. In our future work, we will focus on dynamic adjustment of UAV flight height and further study the collaborative relay of multiple UAVs to improve the quality and efficiency of emergency communication system.

Acknowledgement. This work was supported in part by the NSF of China under Grants 71171045 and 61772130, in part by the Fundamental Research Funds for the Central Universities NO.2232020A-12, in part by the Innovation Program of Shanghai Municipal Education Commission under Grant No. 14YZ130, in part by the International S&T Cooperation Program of Shanghai Science and Technology Commission under Grant No. 15220710600, in part by the Fundamental Research Funds for the Central Universities NO.17D310404, and in part by the Special Project Funding for the

Shanghai Municipal Commission of Economy and Information Civil-Military Inoculation Project “Big Data Management System of UAVs” under the Grant NO.JMRH-2018-1042.

References

1. Arafat, M.Y., Moh, S.: Localization and clustering based on swarm intelligence in UAV networks for emergency communications. *IEEE IoT J.* **6**(5), 8958–8976 (2019). <https://doi.org/10.1109/JIOT.2019.2925567>
2. Feng, G., Wang, C., Li, B., Lv, H., Zhuang, X., Lv, H., Wang, H., Hu, X.: UAV-assisted wireless relay networks for mobile offloading and trajectory optimization. *Peer-to-Peer Netw. Appl.* **12**(6), 1820–1834 (2019). <https://doi.org/10.1007/s12083-019-00793-5>
3. Samir, M., Sharafeddine, S., Assi, C.M., Nguyen, T.M., Ghayeb, A.: UAV trajectory planning for data collection from time-constrained IoT devices. *IEEE Trans. Wirel. Commun.* **19**(1), 34–46 (2020). <https://doi.org/10.1109/TWC.2019.2940447>
4. Zeng, Y., Zhang, R., Lim, T.J.: Wireless communications with unmanned aerial vehicles: opportunities and challenges. *IEEE Commun. Mag.* **54**(5), 36–42 (2016). <https://doi.org/10.1109/MCOM.2016.7470933>
5. Alzenad, M., El-Keyi, A., Yanikomeroglu, H.: 3-D placement of an unmanned aerial vehicle base station for maximum coverage of users with different QoS requirements. *IEEE Wirel. Commun. Lett.* **7**(1), 38–41 (2018). <https://doi.org/10.1109/LWC.2017.2752161>
6. Alzenad, M., Yanikomeroglu, H.: Coverage and rate analysis for unmanned aerial vehicle base stations with LoS/NLoS propagation. In: 2018 IEEE Globecom Workshops (GC Wkshps), pp. 1–7 (2018)
7. Guo, Z., Wei, Z., Feng, Z., Fan, N.: Coverage probability of multiple UAVs supported ground network. *Electron. Lett.* **53**(13), 885–887 (2017). <https://doi.org/10.1049/el.2017.0800>
8. Mozaffari, M., Saad, W., Bennis, M., Debbah, M.: Unmanned aerial vehicle with underlaid device-to-device communications: performance and tradeoffs. *IEEE Trans. Commun.* **15**(6), 3949–3963 (2016). <https://doi.org/10.1109/TWC.2016.2531652>
9. Zhang, S., Liu, J.: Analysis and optimization of multiple unmanned aerial vehicle-assisted communications in post-disaster areas. *IEEE Trans. Veh. Technol.* **67**(12), 12049–12060 (2018). <https://doi.org/10.1109/TVT.2018.2871614>
10. Wang, X., Gursoy, M.C.: Coverage analysis for energy-harvesting UAV-assisted mmWave cellular networks. *IEEE J. Sel. Areas Commun.* **37**(12), 2832–2850 (2019). <https://doi.org/10.1109/JSAC.2019.2947929>
11. Saeedi, A., Azizi, A., Mokari, N.: Throughput maximization in poisson aerial base station based networks with coverage probability and power density constraints. *Trans. Emerg. Telecommun. Technol.* **29**(8), e3456 (2018)
12. Zeng, Y., Zhang, R.: Energy-efficient UAV communication with trajectory optimization. *IEEE Trans. Wirel. Commun.* **16**(6), 3747–3760 (2017). <https://doi.org/10.1109/TWC.2017.2688328>
13. Zhou, L., Yang, Z., Zhou, S., Zhang, W.: Coverage probability analysis of UAV cellular networks in urban environments. In: 2018 IEEE International Conference on Communications Workshops (ICC Workshops), Kansas City, MO, pp. 1–6 (2018). <https://doi.org/10.1109/ICCW.2018.8403633>